PCCP
Physical Chemistry Chemical Physics

Accepted Manuscript

This article can be cited before page numbers have been issued, to do this please use: M. Blancafort-Jorquera and M. Gonzalez, *Phys. Chem. Chem. Phys.*, 2021, DOI: 10.1039/D1CP03629G.

ROYAL SOCIETY OF CHEMISTRY

rsc.li/pccp

Vibrational energy relaxation of a diatomic molecule in a superfluid liquid helium nanodroplet. Influence of the nanodroplet size, interaction energy and energy gap

Miquel Blancafort-Jorquera and Miguel González*

Departament de Ciència dels Materials i Química Física and IQTC, Universitat de Barcelona, Martí i Franquès, 1-11, 08028 Barcelona, Spain

Abstract

The influence of the nanodroplet size, molecule-helium interaction potential energy and v=1-v=0 vibrational energy gap on the vibrational energy relaxation (VER) of a diatomic molecule (X_2) in a superfluid helium nanodroplet [HeND or $(^4He)_N$; finite quantum solvent at T=0.37 K] has been studied using a hybrid quantum approach recently proposed by us and taking as a reference the VER results on the $I_2@(^4He)_{100}$ doped nanodroplet (Vilà et al., *Phys. Chem. Chem. Phys.,* 2018, **20,** 118, which corresponds to the first theoretical study on the VER of molecules embedded a HeND). This has allowed us to obtain a deeper insight into the vibrational relaxation dynamics. The nanodroplet size has a very small effect on the VER, as this process mainly depends on the interaction between the molecule and the nanodroplet first solvation shell. Regarding the interaction potential energy and the energy gap, both factors play an important and comparable role on the VER time properties (global relaxation time, lifetime and transition time). As the former becomes stronger the relaxation time properties decrease in a significant way (the inverse of them follows a linear dependence with respect to the v=1-v=0 coupling term) and they also decrease in an important manner when the energy gap diminishes (linear dependence with the v=1-v=0 energy difference). We expect that this study will motivate further work on the vibrational relaxation process in the HeNDs quantum solvent.

View Article Online
DOI: 10.1039/D1CP03629G

Keywords: superfluid helium nanodroplet, diatomic molecule, vibrational energy relaxation, time dependent DFT, time dependent quantum dynamics, influence of nanodroplet size, influence of vibrational frequency, influence of interaction potential energy.

***** Corresp. author: E-mail: miguel.gonzalez@ub.edu; Fax: +34934021231.

1. Introduction

Vibrational energy relaxation (VER) is one of the most important molecular relaxations, apart from electronic relaxation, in chemical reactivity.[1] VER can take place through two different ways: by energy exchange with other atoms/molecules and by exchanging energy with other degrees of freedom of the same molecule (intramolecular vibrational relaxation).

The mechanism of VER depends on the phase in which the molecules are located. In gas phase, vibrational relaxation happens in a not very efficient manner by means of binary molecular collisions. In contrast to this, in condensed phases the number of molecules surrounding the vibrationally excited molecule is larger, so that the exchange of energy becomes much easier.[2,3] Besides, the study of the VER processes in condensed phase also allows to obtain information on the liquid phase structure, intermolecular dynamics and solute-solvent interactions.[4]

Ultrafast time-resolved spectroscopic techniques have extensively contributed to the knowledge of the VER mechanism in the condensed phase.[5,6] Pump (excite)-probe (detect) schemes are the most used spectroscopic techniques (a first ultrashort laser pulse excites the molecules and a delayed second pulse probes the vibrational populations).[2,3,7] Depending on the system under consideration, the ways to pump and probe may be different:[8] in general, excitation involves stimulated Raman scattering or infrared (IR) absorption, and the probe depends on the type of experiment. In phase coherence experiments, sub-picosecond IR pump-probe spectroscopy as well as coherent anti-Stokes Raman spectroscopy and photon echo are used to study VER.[9]

Several theoretical approaches have been developed to investigate VER in condensed phase. Using classical mechanics the friction exerted by the liquid on the vibrational motion of the solvated molecule damps its amplitude while heating the bath.[10] A Langevin equation for a damped oscillator subject to a fluctuation force is applied here and relaxation takes place efficiently when the excited oscillator and solvent fluctuation frequencies coincide. This classical approach is suitable for low frequencies or high temperatures.

The first order time dependent perturbation theory is the simplest quantum approach to calculate the rate constant for the transition between two vibrational levels

View Article Online
DOI: 10.1039/D1CP03629G

(through the Fourier transform of the time correlation function of the interaction energy). The quantum time correlation function, in general is not available due to the large number of solvent molecules, so approximate treatments are needed. One way to proceed is finding the classical analogous for the rate constant equation considering the detailed balance principle and the equivalence between the classical and real parts of the quantum correlation functions.[2] Then, the classical correlation function is derived from molecular dynamics (MD) simulations. Another way to treat this is by modelling the liquid as a bath of independent harmonic oscillators and then calculate the corresponding quantum correlation function.[11]

Finally, another theoretical approach is based on the real-time simulation of the VER dynamics, which has only been possible for a classical non-equilibrium MD coupled to quantum oscillators.[5,6,10] This strategy is highly demanding due to the large number of solvent molecules and the different time scales involved.

Here, in the context of superfluid ^{4}He nanodroplets (HeND; finite quantum solvent at $T = 0.37$ K),[12,13,14,15] we have considered real-time simulations of the VER employing a full quantum treatment of the system, which is formed by a homonuclear diatomic molecule (X_2) embedded in a HeND. This has been achieved using a hybrid approach proposed by our group,[16] which is based in a previous work of our own[17] and includes significant modifications in the mathematical procedure used in the time-propagation of the wave functions. These modifications are very relevant as the VER in HeND is a very slow process. In the first theoretical study of VER in HeNDs the $I_2(X)$ diatomic molecule was investigated[16] and the main goal of the present study is to obtain a deeper insight into the VER dynamics using this molecule as reference system. These quantum simulations have been feasible thanks to the use of the time dependent density functional theory (TDDFT) for the description of superfluid helium.

The hybrid method mentioned above has also allowed us to study the dynamics of different physico-chemical processes involving HeNDs (photodissociation of diatomics,[17,18,19] capture of atoms,[20,21] dimerization reactions,[22,23] vibrational energy relaxation,[16] rotational energy relaxation[24,25] and HeND relaxation[26]). This method could also be applied to investigate electronically non-adiabatic bimolecular reactions (e.g., electron transfer reactions[27]) if the electronic states and couplings are known.

View Article Online
DOI: 10.1039/D1CP03629G

The interest in HeNDs resides in their special properties such as superfluidity, chemical inert character and finite size, which have led to important applications in the field of Chemical Physics/Physical Chemistry,[12,13,14,15] such as high resolution spectroscopy of atoms and molecules, stabilisation of metastable species, and the synthesis of metal nanoparticles[28,29,30,31,32] and nanowires.[33,34]

Regarding the I_2 molecule in the electronic ground state (benchmark system), its high-resolution rovibrational spectroscopy has been widely investigated in several contexts.[35,36,37,38,39,40,41,42,43] The energy separation between two consecutive vibrational levels of $I_2(X)$ is quite small, $\nu_e = 214.502\ \mathrm{cm}^{-1}$ (308.621 K),[44] which provides a high density of vibrational states. This leads to relatively fast VER rates in comparison to other molecules, making this system particularly attractive to be studied. Thus, e.g., the VER of $I_2(X)$ has been examined in gas phase (He-$I_2(X)$ mainly[45,46,47]) and condensed media such as mesitylene[48] and liquid Xe.[49,50,51,52,53,54,55,56,57,58,59,60]

Rovibrational spectroscopy has been well studied in HeNDs[12,13,14] and this solvent induces small band broadening and vibrational line shifts (typically less than 2 cm^{-1}). As the interaction with the helium solvent is weak the vibrational symmetry of the molecule is not modified in liquid helium. However, only a few studies have been reported on the VER of molecules in helium nanodroplets and they consider, e.g., IR spectroscopy and bolometric detection of some molecules and binary complexes.[61,62,63,64]

The VER of HF($\nu = 1$) in HeNDs is very slow ($t \geq 0.5$ ms)[63] due to its large vibrational energy gap ($\nu_e = 4138.32\ \mathrm{cm}^{-1}$ (5954.12 K)),[44] which leads to an important metastability. The nanodroplet size dependent line shifts and broadening indicate that the coupling of the HF vibration with the HeND surface excitations (ripplons) is the main relaxation mechanism.[63] For binary complexes of HF such as Ne, Ar, Kr-HF(ν), the relaxation takes place in similar time scales to the HF case and the relaxation rate is also size dependent.[64]

Furthermore, the vibrational relaxation and dephasing of some alkali dimers (Rb_2, Na_2 and K_2) placed in a dimple on the surface of a HeND[65,66,67] and the photoinduced non-adiabatic dynamics of Na_3 and K_3 in quartet states (also formed on the HeND

View Article Online
DOI: 10.1039/D1CP03629G

surface) have been also studied,[68] providing information on the $Na_3(2^4E')$ VER. Besides, the de-alignment of the $I_2(X)$ rotation in HeNDs has been also reported.[69]

This chapter is organised as follows. The hybrid quantum method employed in the simulation of the real-time VER dynamics is described in Section 2. The main results obtained for the different initial conditions explored are presented and discussed in Section 3. The summary and conclusions are given in Section 4. Finally, some additional information is included in the Electronic Supplementary Information (ESI) document.

2. Theoretical methods

As the same methodology used in ref. 16 has been employed here, a shorter description of the main aspects is given in this section. At the low temperature of the HeNDs ($T = 0.37\ K$) only the vibrational ground state ($v = 0$) of the molecule is populated in the thermal equilibrium. The zero time condition of the dynamics is then represented by the helium wave function corresponding to the $I_2(X,v=0)@^4He_N$ ground state doped nanodroplet, but with a sudden change of the I_2 vibrational wave function from v=0 to the first excited vibrational level (v=1). The global vibrational relaxation process can be represented as:

$$I_2(X, v = 0)@^4He_N + h\nu \rightarrow \left[I_2(X, v = 1)@^4He_N\right]^* + h\nu'$$

$$\left[I_2(X, v = 1)@^4He_N\right]^* \rightarrow \left[I_2(X, v = 0)@^4He_{N'}\right]^* + (N - N')^4He \quad (1)$$

, where the vibrational relaxation time does not necessarily coincide with the liquid helium relaxation time.

The impurity is placed in the centre of the nanodroplet since the strength of the I_2-He interaction is larger than that of the He-He interaction. This fact and the symmetry of the system allows us keeping frozen the I_2 centre of mass (CM) during the VER dynamics.[16,17] Furthermore, as the mass of the I_2 CM is much larger than that of a He atom its classical description is justified (i.e., the zero-point motion of the I_2 CM is not considered). Besides, in this study the rotational degrees of freedom of the molecule have not been taken into account.

View Article Online
DOI: 10.1039/D1CP03629G

The real-time quantum simulations of the VER have been performed following a "divide and conquer" mean field hybrid strategy, combining a commonly used method to study rather large systems of bosonic superfluid liquid ^{4}He (TDDFT)[16,17,18,19,20,21,22,26,70,71,72,73] and a usual method to study atoms and molecules in gas phase (time dependent wave function).[16,17,18,19, 20 ,22]

In the TDDFT calculations the Orsay Trento (OT) phenomenological density functional[74] has been used, and the non-local contributions to the helium correlation energy and the back-flow terms have been neglected for computational reasons, as usual.[16,17,18,19,20,21,22,23,24,26,70,71,72,73] Moreover, a modification has been added to the OT functional in order to avoid unphysical helium densities when the interaction between the dopant molecule and helium is strong.[75] The X_2 vibrational degree of freedom has been described using standard quantum mechanics, employing suitable time dependent wave functions.

Using this hybrid approach the equations of motion are found by minimising the quantum action ($\mathcal{A}$):

$$\mathcal{A}[\Psi_{He},\varphi_{X_2}] = \int dt\left\{E[\Psi_{He},\varphi_{X_2}] - i\hbar\int d\boldsymbol{R_{He}}\Psi^*_{He}(\boldsymbol{R_{He}},t)\frac{\partial}{\partial t}\Psi_{He}(\boldsymbol{R_{He}},t) - i\hbar\int dr\varphi^*_{X_2}(r,t)\frac{\partial}{\partial t}\varphi_{X_2}(r,t)\right\} \quad (2)$$

, where $\Psi_{He}(\boldsymbol{R_{He}},t)$ is the complex effective wave function describing the liquid helium ($|\Psi_{He}(\boldsymbol{R_{He}},t)|^2 \equiv \rho_{He}(\boldsymbol{R_{He}},t)$), $\varphi_{X_2}(r,t)$ is the vibrational wave function of the molecule and E is the total energy of the system.

The quantum action must be minimised, by taking variations with respect to each one of the wave functions, to obtain two coupled time dependent Schrödinger-like nonlinear equations that rule the evolution of helium and the diatomic molecule respectively:

$$i\hbar\frac{\partial}{\partial t}\Psi_{He}(\boldsymbol{R_{He}},t) = \left[-\frac{\hbar^2}{2m_{He}}\nabla^2 + \int dr V_{He-X_2}(r,\boldsymbol{R_{He}})|\varphi_{X_2}(r,t)|^2 + \frac{\delta\varepsilon_c[\rho_{He}]}{\delta\rho_{He}}\right]\Psi_{He}(\boldsymbol{R_{He}},t) \quad (3)$$

$$i\hbar\frac{\partial}{\partial t}\varphi_{X_2}(r,t) = \left[-\frac{\hbar^2}{2\mu_{X_2}}\frac{\partial^2}{\partial r^2} + \int d\boldsymbol{R_{He}} V_{He-X_2}(r,\boldsymbol{R_{He}})\rho(\boldsymbol{R_{He}},t) + V_{X_2}(r)\right]\varphi_{X_2}(r,t) \quad (4)$$

, where μ_{X_2} is the reduced mass of X_2. The $\varepsilon_c[\rho_{He}]$ term corresponds to the potential energy and correlation energy densities of superfluid liquid helium. The term $V_{He-X_2}(r,\boldsymbol{R_{He}})$ stands for the interaction potential energy between a He atom and the X_2 molecule, which has been taken from ref. 76. Due to the key role played by the He-molecule interaction, it is highly relevant to calculate it accurately, which is a difficult task as it is dispersion dominated. For the $V_{I_2}(r)$ potential energy curve describing the interaction between the two atoms of the molecule, a Morse function (eq. (5)) with the experimental parameters from ref. 44 ($r_e = 2.6663$ Å, $D_e = 18052.42\ K$ and $a = 1.857608$ Å^{-1}) has been employed, where this function is given by

$$V_{I_2}(r) = D_e\left(1 - e^{-a(r-r_e)}\right)^2 \tag{5}$$

Equations (3) and (4) are identical to those employed in the photodissociation of Cl_2(B←X) in HeNDs.[17] However, this process is very different from VER, where the relative coordinate wave function is always placed around the equilibrium distance, r_e, of the X_2 potential energy curve. For this reason we have applied a much more efficient mathematical strategy to determine the time evolution of the system.[16] Thus, the $\varphi_{X_2}(r)$ vibrational wave function has been expressed as a linear combination of the vibrational eigenfunctions basis set $\{\varphi_i(r)\}$ of the vibrational Hamiltonian operator of the isolated molecule:

$$\varphi_{X_2}(r) = \sum_i c_i \varphi_i(r) \tag{6}$$

Equation (4) can now be transformed into equation (8) (see below), which can be solved in a more efficient way in terms of numerical accuracy and computational time. Then, to describe the VER dynamics the following equations have been propagated in time:

$$i\hbar\frac{\partial}{\partial t}\Psi_{He}(\boldsymbol{R_{He}},t) = \left[-\frac{\hbar^2}{2m_{He}}\nabla^2 + \sum_{i,j} c_i^*(t)c_j(t)V_{ij}(\boldsymbol{R_{He}}) + \frac{\delta\varepsilon_c[\rho_{He}]}{\delta\rho_{He}}\right]\Psi_{He}(\boldsymbol{R_{He}},t) \tag{7}$$

$$i\hbar\frac{dc_i(t)}{dt} = E_{vib,i}c_i(t) + \sum_j c_j(t)V_{ij} \tag{8}$$

View Article Online
DOI: 10.1039/D1CP03629G

$$i, j = 0, 1, 2, \ldots n$$

, where $\{E_{vib,i}\}$ are the corresponding vibrational energy eigenvalues, and the helium coordinate-dependent potential energy matrix elements, $V_{ij}(\boldsymbol{R_{He}})$, are equal to

$$V_{ij}(\boldsymbol{R_{He}}) \equiv \langle i \left| V_{He-X_2} \right| j \rangle = \int dr V_{He-X_2}(r, \boldsymbol{R_{He}}) \varphi_i^*(r) \varphi_j(r) \quad (9)$$

and

$$V_{ij} \equiv \left\langle i \left| \int d\boldsymbol{R_{He}} V_{He-X_2}(r, \boldsymbol{R_{He}}) \rho_{He}(\boldsymbol{R_{He}}, t) \right| j \right\rangle \quad (10)$$

To converge the calculations for the initial excited vibrational level $v = 1$, it has been enough to include in the calculations all vibrational levels from $v = 0$ up to $v_{max} = v + 3$ (*i.e.*, $v_{max} = 4$ in this case).

The determination of the initial time ground state $I_2(X, v = 0)@^4He_N$ configuration has been obtained by finding the stationary solution of eq. (7) but keeping fixed the vibrational wave function to the $v = 0$ one ($c_0 = 1, c_i = 0, i \neq 0$). This approximation is acceptable due to the large differences between the involved energies (I_2 chemical bond versus van der Waals (vdW) I_2-He interaction), and has been validated in the dynamical calculations (the wave function $\varphi_{X_2}(r)$ that corresponds to the global relaxation time is just equal to $\varphi_0(r)$).

Equation (7) has been solved numerically discretising the space in a grid of points in which the spatial derivatives of the kinetic energy terms have been calculated using the fast Fourier transform (FFT).[77] The numerical time propagation has been performed employing a fifth order predictor-corrector method,[78] preceded (first three initial steps) by a fourth order Runge-Kutta method[79] (time step=1.0×10^{-3} ps).

The Cartesian grid for the helium wave function has a spacing of 0.40 Å for the x and y axes and of 0.30 Å for the z axis, where the molecule is placed, and each axis has a total length of 38.0 Å (Figure 1). As in our previous works, a quartic negative imaginary potential (NIP)[80] energy term has been defined at the edges of the grid. Thanks to its complex character it gradually absorbs possible fragments of the helium wave function arising from the evaporation of helium, avoiding in this way artificial reflections at the edges. This additional potential energy term, which is placed inside the parentheses of

View Article Online
DOI: 10.1039/D1CP03629G

the right hand side of equation (7) and only acts at the edges of the grid, has the following expression:[80]

$$V_{NIP} = -iA\frac{5}{2}\left(\frac{d - d_{NIP}}{L}\right)^4 \quad (11)$$

, where the absorption strength (A) is equal to 331.0 K, the length (L) has a value of 1.0 Å, and the NIP has been placed (d_{NIP}) at a distance of 1.0 Å before the limit of the helium grid.

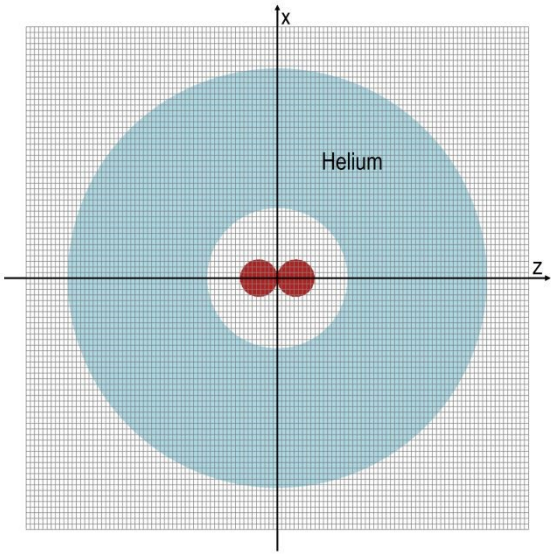

Figure 1. Schematic plot of the Cartesian grid used for the helium wave function showing the discretization in the xz plane. The blue area shows the region where the helium density takes non-negligible values and the red circles represent the diatomic molecule in the equilibrium geometry.

The numerical time propagation of equation (8) takes benefit from the basis set expansion of $\varphi_{X_2}(r)$. For the evaluation of the required integrals the basis set functions have been discretised into a grid of 1000 points between r=2.3 Å and 3.5 Å. To integrate in time, for each time step $t \rightarrow t + \delta t$ the full Hamiltonian of the diatomic molecule (eq. (8)) is diagonalized, and the time evolution from t to $t + \delta t$ is determined in terms of the stationary states $\{|\alpha\rangle\}$ for time t. Then, we come back to the original basis set, $\{|i\rangle\}$, and the procedure is repeated for the new time, $t + \delta t$, to determine the evolution to $t + 2\delta t$, and so on.[16]

View Article Online
DOI: 10.1039/D1CP03629G

3. Results and discussion

To analyse the influence of the nanodroplet size, molecule-helium interaction potential energy and $v = 1$- $v = 0$ vibrational energy separation on the VER, a number of simulations have been performed. These properties have been modified conveniently taking as a reference the VER results, from $v = 1$ to $v = 0$, of a I_2(X) molecule embedded in a nanodroplet of 100 ^{4}He atoms.[16]

For the study of the effect of the nanodroplet size the number of ^{4}He atoms has been taken as equal to N=50, 100, 150 and 200. For the analysis of the influence of the molecule-nanodroplet interaction the I_2-He interaction potential energy has been multiplied by several scalar factors: $V = xV_{I_2-He}$ with x=1.50, 1.25, 1.00, 0.75 and 0.50 (N=100). Concerning the effect of the vibrational energy separation it has been modified changing the equilibrium frequency of the oscillator, ν_e: $\nu_e = x\,\nu_{e,I_2}$ with x=1.50, 1.25, 1.00 and 0.75 (N=100), where the vibrational energy is given by $E_{vib}(v) = h\nu_e\left(v+\frac{1}{2}\right) - h\nu_e x_e\left(v+\frac{1}{2}\right)^2$.

3.1. Vibrational relaxation vs. nanodroplet size

The helium density of the I_2(X,v=0)@^4He_N system in the ground state for nanodroplets of different sizes (N=50, 100, 150 and 200) is shown in Figure 2. The nanodroplet size has a very small effect on the vibrational energy relaxation (Figure 3). This happens in this way because the interaction energy of the molecule with the nanodroplet mainly comes from the first solvation layer, which is substantially large in comparison to the other ones and is completely defined for all the nanodroplet sizes (Figure 2), due to the relatively strong I_2-He interaction. Moreover, the I_2-helium interaction energy tends to converge into a limit value, taking the following values at t=0 (i.e., just when the sudden excitation to v=1 takes place): -664.1, -740.0, -767.6 and -782.7 K for N=50, 100, 150 and 200, respectively. Information about all the energies involved is given in Table s1.

View Article Online
DOI: 10.1039/D1CP03629G

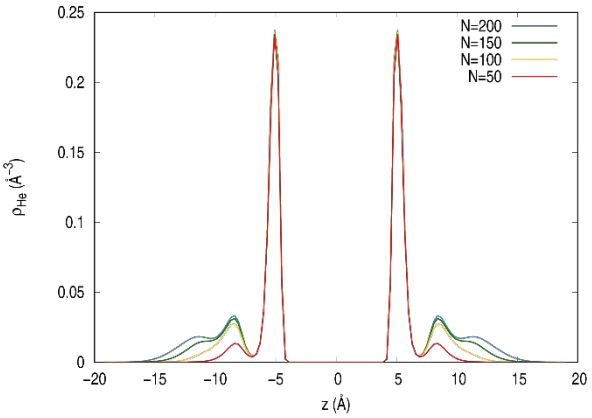

Figure 2. Helium density of the $I_2(X,v=0)@^4He_N$ nanodroplet in the ground state, along the molecular axis (z axis), for N=50, 100, 150 and 200.

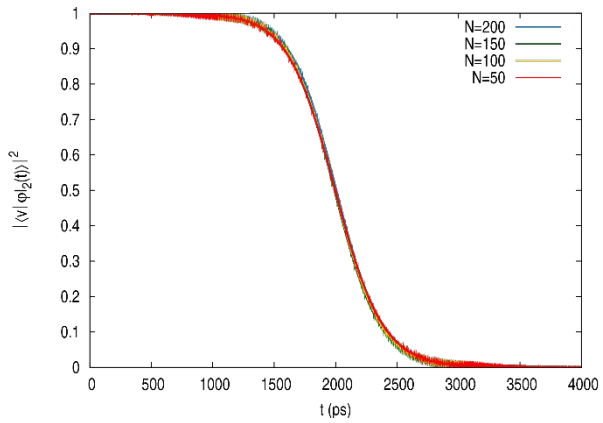

Figure 3. Population of the $v=1$ excited vibrational state as a function of time for N=50, 100, 150 and 200.

3.2. Vibrational energy relaxation vs. I_2-He interaction potential

Here, the nanodroplet with N=100 has been considered. The shape of the nanodroplet helium density is quite affected by the "I_2-He" interaction potential energies selected (Figure 4). For the stronger interaction potential energies higher peaks (densities) are observed for the first and second solvation shells, while the nanodroplet radius (~15 Å) is essentially not affected by the interaction energy.

View Article Online
DOI: 10.1039/D1CP03629G

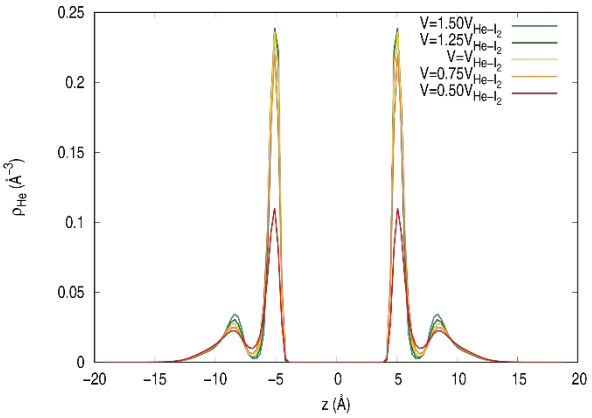

Figure 4. Helium density of the $I_2(X,v=0)@^4He_{100}$ nanodroplet in the ground state along the molecular axis (z axis) for $V = xV_{I_2\text{ - He}}$ with x=1.50, 1.25, 1.00, 0.75 and 0.50.

Vibrational relaxation is clearly faster for the stronger "I_2-He" interaction potential energies (Figure 5). The time scales involved in the vibrational relaxation from v=1 to v =0 for the five selected "I_2-He" interaction potential energies are shown in Table 1 and Figure 6. The global relaxation time is defined as the time it takes for the whole vibrational relaxation to occur, this is from t=0 to the time at which the population of the excited vibrational state is equal to 1%; the lifetime is taken from t=0 to the time at which the population of this state is 50%; and the transition time is the time needed for the population of the excited state to decrease from 99 to 1%. The values of the three relaxation times decrease in a substantial way with increasing the strength of the interaction energy and tend towards an asymptotic behaviour. More concretely, taking as a reference the results for x=1.00, the lifetime is equal to 4.87, 1.84, 1.00. 0.40 and 0.21 for x=0.50, 0.75, 1.00, 1.25 and 1.50 respectively, and similar values are obtained for the other relaxation times (with the only exception of the transition time for x=0.50 (3.88)). These results will be interpreted at the end of this subsection.

The time evolution of the different energies and the number of helium atoms of the HeND are shown in Figure 7 and their corresponding increments with respect to t=0 values are presented in Figure s1. The temporal evolution of the vibrational energy implied in the VER process follows the same pattern with respect to the changes in the "I_2-He" interaction potential as the population of the v=1 excited state, and it changes from 460 to 154 K. The helium nanodroplet energy increases ≈4.0-6.4 K during the relaxation, as a result of the evaporation of a single ^{4}He atom (please, see the explanation given at the end of subsection 3.3). The interaction energy between the

diatomic molecule and the helium nanodroplet changes very little as a result of the relaxation process (of the order of 0.1 K), as the helium nanodroplet structure is essentially not affected. Only small amplitude oscillations of the interaction energy can be seen during the transitions which vary from ≈ -3.2 to 4.4 K and ≈ -0.4 to 0.8 K, from the stronger to weaker interaction potential energies, respectively. As a result of the vibrational relaxation, for the simulated times the total energy of the doped nanodroplet decreases ≈300 K in all cases.

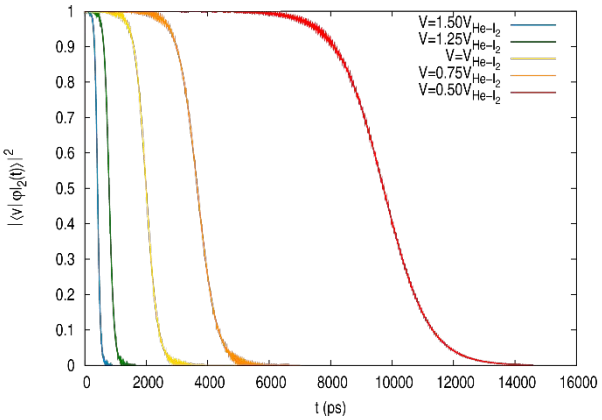

Figure 5. Populations of the v=1 excited vibrational state as a function of time for $V = xV_{I_2\text{ - He}}$, with x=1.50, 1.25, 1.00, 0.75 and 0.50 (N=100).

The expected value of the V_{01}^2 coupling term during the transition time, $\langle V_{01}^2 \rangle$, as a function of the interaction potential energy is presented in Table s2. It can be seen that $\langle V_{01}^2 \rangle$ increases in a significant way with the interaction energy. Thus, e.g., when the interaction energy is increased 50% with respect to the reference one (x=1.00) the coupling term increases by a factor of 3.84, while when it is decreased 50% with respect to the reference the coupling term decreases by a factor of 10.4 (Table s2). From the analysis of the inverse of the values of the relaxation times as a function of $\langle V_{01}^2 \rangle$, it comes out that there is an approximate linear relation between these properties and $\langle V_{01}^2 \rangle$ (Figure 8). This linear dependence agrees with that given by the Fermi's Golden Rule for the transition probability between two states.[81]

View Article Online
DOI: 10.1039/D1CP03629G

Table 1. Global relaxation times, lifetimes and transition times of the v=1 excited vibrational state for the five "I_2-He" potential energies considered ($V = xV_{I_2\text{-}He}$) and N=100.[a]

x	Global relax. time (ps)	Lifetime (ps)	Transition time (ps)
0.50	13060 (4.55)	9721 (4.87)	6705 (3.88)
0.75	5094 (1.77)	3661 (1.84)	2856 (1.65)
1.00	2873 (1.00)	1995 (1.00)	1726 (1.00)
1.25	1176 (0.41)	789 (0.40)	748 (0.43)
1.50	640 (0.22)	413 (0.21)	432 (0.25)

[a]The relaxation times relative to the x=1.00 reference case are given between parentheses.

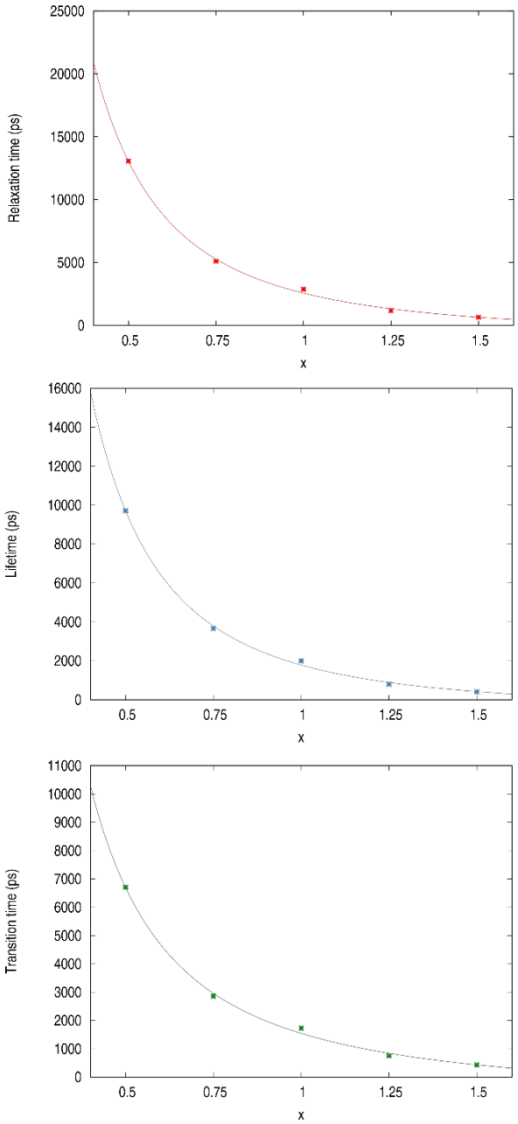

Figure 6. Global relaxation times (top), lifetimes (middle) and transition times (bottom) of the v =1 excited vibrational state, as a function of x ($V = xV_{I_2\text{-}He}$), and fitting curve (quadratic polynomial) for N=100.

View Article Online
DOI: 10.1039/D1CP03629G

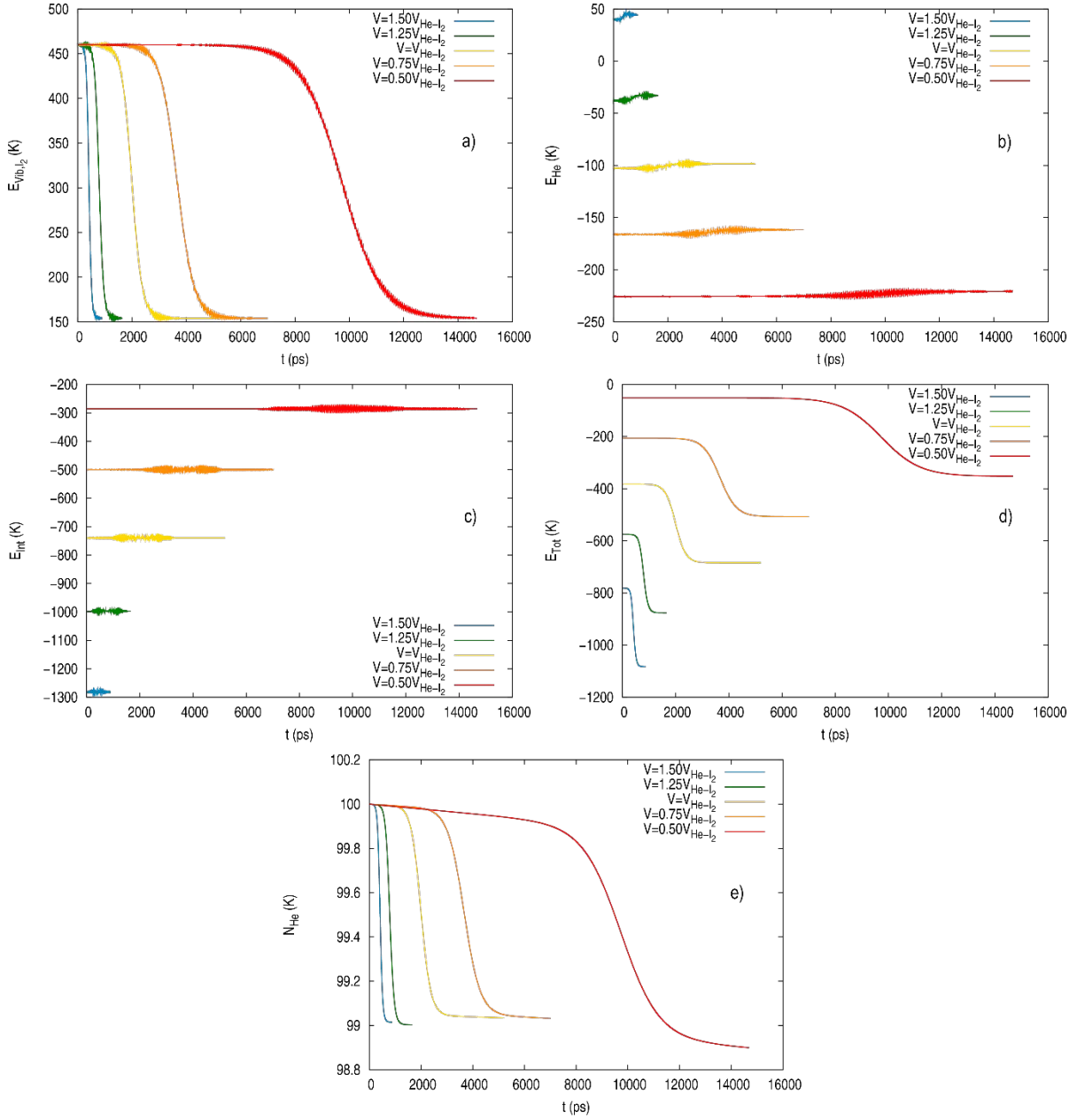

Figure 7. Energies involved in the VER from v=1 at the five selected "I_2-HeND" interaction potential energies and number of ^{4}He atoms of the nanodroplet, as a function of time for N=100: a) vibrational energy of the molecule; b) energy of the helium nanodroplet; c) molecule-nanodroplet interaction energy; d) total energy of the system (I_2@HeND); e) number of ^{4}He atoms of the HeND.

View Article Online
DOI: 10.1039/D1CP03629G

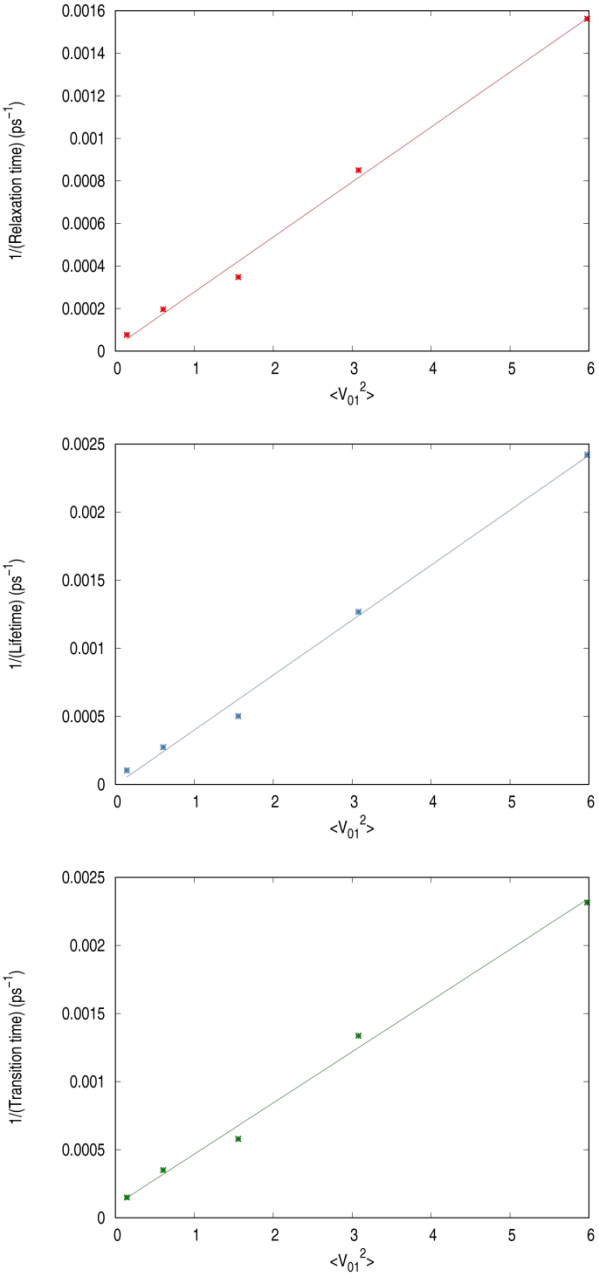

Figure 8. Inverse of the global relaxation times (top), lifetimes (middle) and transition times (bottom) of the v=1 excited vibrational state, as a function of the $\langle V_{01}^2 \rangle$ coupling term for the different interaction potential energies ($V = xV_{I_2\text{-}He}$, with x=0.75, 1.00, 1.25 and 1.50) and N=100. The coupling term increases with x.

3.3. Vibrational relaxation vs. energy gap

Changes in the oscillator frequency affect the energies of the vibrational levels and the gaps between them, and the energy gaps between the $|v=1\rangle$ and $|v=0\rangle$ vibrational states of the molecule take the following values: $\Delta E_{vib,1-0} = 230$, 306, 382 and 457 K for the $\nu_e = 0.75\nu_{e,I_2}$, $1.00\nu_{e,I_2}$,$1.25\nu_{e,I_2}$ and $1.50\nu_{e,I_2}$ frequency values analysed, respectively. The increase of the energy separation between the v=1 and v=0 vibrational levels is expected to quench somehow the vibrational relaxation process, as in fact has been found here.

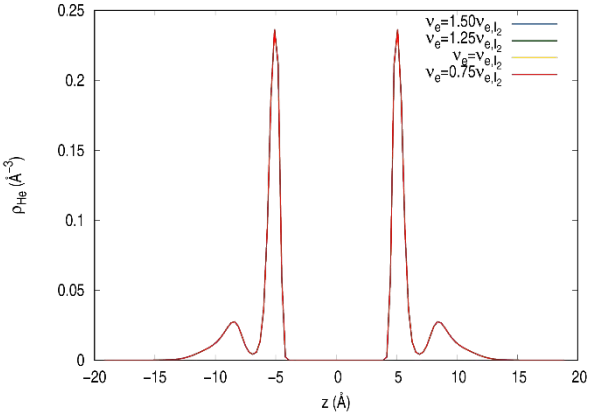

Figure 9. Helium density of the $I_2(X,v=0)@^4He_{100}$ nanodroplet in the ground state along the molecular axis (z axis) for $\nu_e = x\,\nu_{e,I_2}$ with x=1.50, 1.25, 1.00 and 0.75.

As in the previous subsection, the nanodroplet with N=100 has also been considered here. The structure of the vibrational wave function is very little affected by the selected equilibrium frequencies of the $I_2(X)$ Morse oscillator, and for this reason the initial helium density is identical for all cases studied (Figure 9). However, the changes in the frequency of the Morse oscillator lead to important modifications in the VER time properties, as it is shown in Figure 10.

The global relaxation times, lifetimes and transition times of the four cases considered are shown in Table 2 and Figure 11. It can be seen that the larger the frequency of the oscillator the slower the relaxation is, following an approximately linear dependence for the interval of frequencies investigated. If we take as a reference the relaxation times obtained when x=1.00, the lifetime values are 0.35, 1.00, 1.90 and 3.05 for x=0.75, 1.00, 1.25 and 1.50, respectively, the other properties taking similar

values (with the exception of the global relaxation and transition times for x=1.50 (2.73 and 2.60, respectively)). These results will be interpreted below.

During the VER analogous patterns are seen in the evolutions of the energies and number of ^{4}He atoms of the nanodroplet, with the transition from v=1 to v=0 being faster for the smaller oscillator frequencies, i.e., for the lower vibrational energy gaps (Figure 12). The vibrational energy of the molecule decreases according to the v=1-v=0 energy gap and the helium energy of the nanodroplet increases ≈4-5 K. The small changes that occur in the interaction energy, from ≈-0.5 to 0.5 K with oscillations of about 3-3.5 K during the transition, denote that the structure of the liquid helium does not change significantly during the VER. Moreover, changes in the total energy of the doped nanodroplet are similar to the vibrational energy released and the final helium energy of the nanodroplet is similar for all cases.

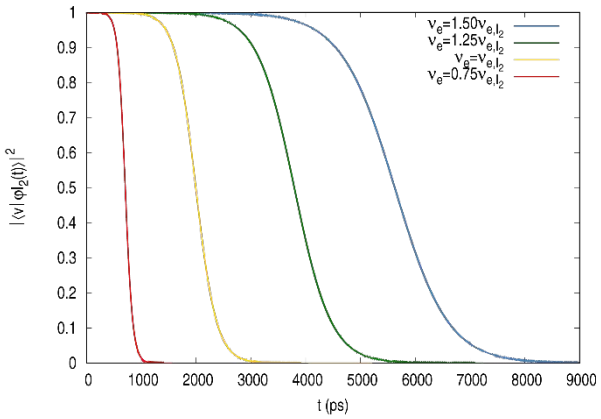

Figure 10. Populations of the v=1 excited vibrational state as a function of time for $\nu_e = \mathrm{x}\,\nu_{e,I_2}$ with x=1.50, 1.25, 1.00 and 0.75 (N=100).

The dependence of the $\langle V_{01}^2 \rangle$ coupling term with respect to the energy gap is presented in Table s3, which shows that it increases moderately with the energy gap, (differing from what happens in the case of the $\langle V_{01}^2 \rangle$ dependence on the interaction energy). According to these $\langle V_{01}^2 \rangle$ values the inverse of the values of the three relaxation times should increase as the energy gap increases. However, from the dynamics results the opposite trend is found. This means that there is another factor that is playing a dominant role here. The results obtained for the rotational relaxation[24] suggest, by analogy, that the expected velocity of the oscillator, $\langle \mathrm{v}_{oscillator}^2 \rangle^{1/2} \propto \nu_e^{\frac{1}{2}}$ (neglecting anharmonicity), could be involved in making the VER process more difficult as it

increases. Unfortunately, the information available does not allow us to characterise the dependence of the time relaxation properties with respect to both $\langle V_{01}^2 \rangle$ and $\nu_e^{1/2}$. Nevertheless, it has been shown before that in the situation under consideration a simple (linear) dependence relates the relaxation times and ν_e (Figure 11).

Table 2. Global relaxation times, lifetimes and transition times of the v=1 excited vibrational state for the four vibrational frequencies ν_e considered ($\nu_e = \mathrm{x}\ \nu_{e,I_2}$) and N=100.[a]

x	Global relax. time (ps)	Lifetime (ps)	Transition time (ps)
0.75	1027 (0.36)	707 (0.35)	628 (0.36)
1.00	2873 (1.00)	1995 (1.00)	1726 (1.00)
1.25	5334 (1.86)	3793 (1.90)	3101 (1.80)
1.50	7842 (2.73)	6079 (3.05)	4493 (2.60)

[a]The relaxation times relative to the x=1.00 reference case are given between parentheses.

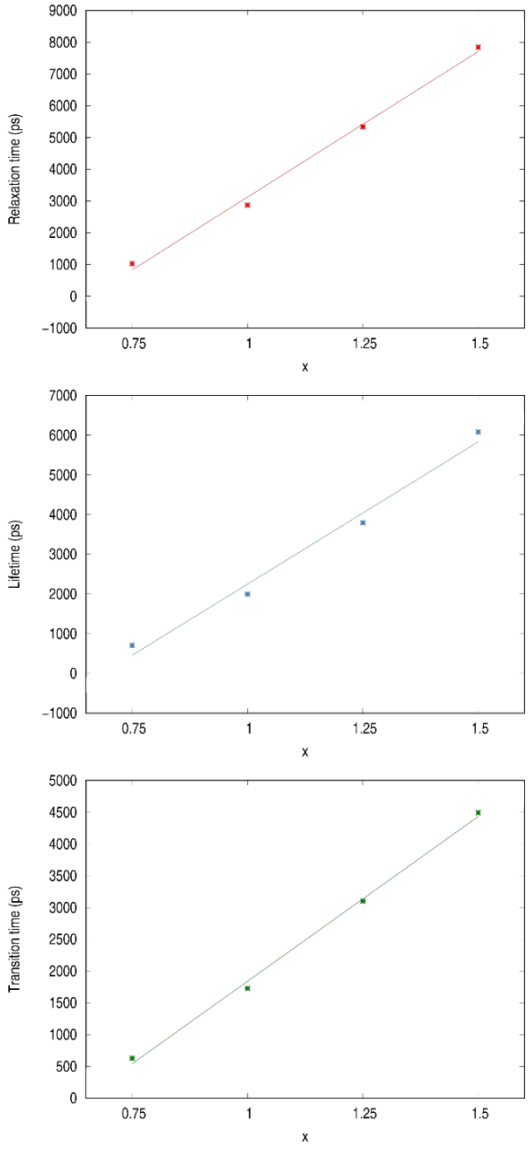

View Article Online
DOI: 10.1039/D1CP03629G

Figure 11. Global relaxation times (top), lifetimes (middle) and transition times (bottom) of the v=1 excited vibrational state, as a function of $x\,(\nu_e = \mathrm{x}\,\nu_{e,I_2})$ for N=100.

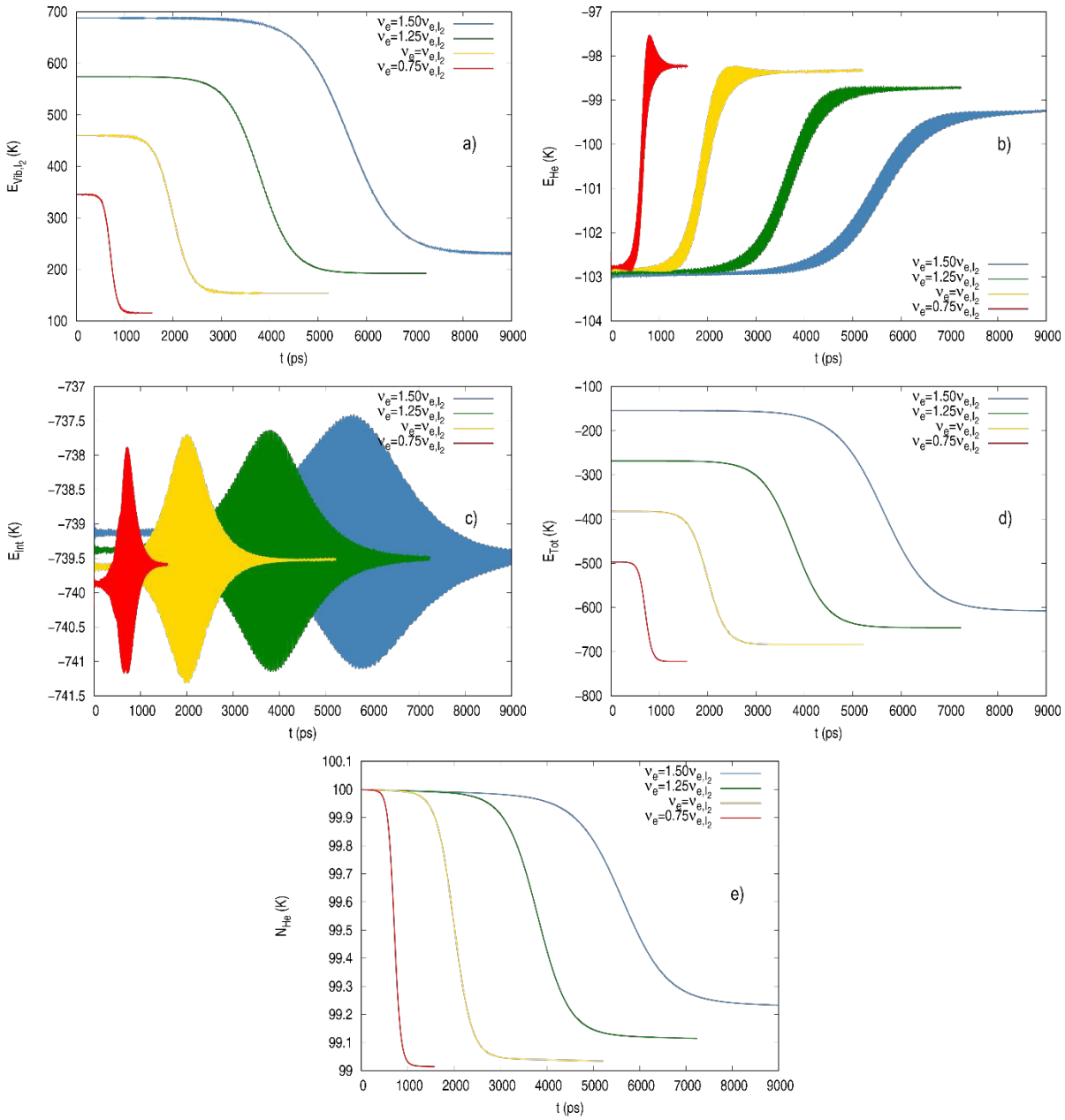

Figure 12. Energies involved in the VER from v=1 at four $\nu_e$vibrational frequencies selected and number of ^{4}He atoms of the nanodroplet, as a function of time for N=100: a) vibrational energy of the molecule; b) energy of the helium nanodroplet; c) molecule-nanodroplet interaction energy; d) total energy of the system (I_2@HeND); e) number of ^{4}He atoms of the HeND.

The single He atom evaporated of the nanodroplet observed in all cases considered in Section 3 contrasts with the larger number of He atoms evaporated that can be estimated, considering the ratio between the vibrational excitation energy to be removed from the HeND and the binding energy of a He atom in the HeND (assuming

View Article Online
DOI: 10.1039/D1CP03629G

that each evaporated atom has a negligible translational kinetic energy), as it has been previously reported and discussed in ref. 16. Furthermore, it should be noted that during the simulations the energy of the system is conserved if we take into account the energy of the evaporated helium atom, but this atom has an excess of energy compared to what would be expected from the experimental evidences.

This fact probably results from the continuous description of the HeND (DFT approach), which nowadays is the only available way to describe the dynamics of physicochemical processes in this superfluid quantum solvent. Besides, we have employed the Orsay-Trento phenomenological density functional,[74] which is the best one available and has been used in all or almost all the dynamics studies reported so far involving HeNDs and atoms/molecules.

Previous studies, where the helium nanodroplets were described using a DFT approach, have shown the evaporation of He atoms in different situations. Thus, in soft landing all He atoms of the nanodroplet were evaporated.[82] Other processes where evaporation was observed include, e.g., atom capture,[20,21] dimerization[22,23] and clustering.[83] However, in these cases the number of evaporated atoms was below the expected value, on the basis of the energy involved in the process and the binding energy of the He atom in a HeND (7.2 K). As in the present work, in all cases the Orsay-Trento functional was used, but in the soft landing this functional was modified to account for the very structured helium arrangements appearing in the collision.[83]

In spite of the previous facts, taking into consideration that within this approach superfluidity is taken into account, that there is an efficient release of the vibrational excitation energy by the helium, and the remarkable fact that vibrational relaxation is mainly affected by the first solvation shell, we believe that the present results are reasonable and represent a good starting point for the study of the influence of the three key aspects examined here on the VER dynamics in HeNDs.

In the future, theoretical efforts should be made in order to improve the description of the evaporation of helium atoms and to take into account the rotational energy. The theoretical results available for the rotational energy relaxation in HeNDs (which strongly depends on the B_e rotational constant and the strength of the molecule-helium interaction[24,25]) suggest that a complex dynamics behaviour can be expected for

View Article Online
DOI: 10.1039/D1CP03629G

the vibro-rotational relaxation of molecules which are not as fast rotors as H_2 and interact with helium in a significantly stronger way than H_2. Thus, e.g., for HCl and isotopologues a complex rotational energy relaxation dynamics has been theoretically found showing non-monotonic dependences of the relaxation times on B_e and with relaxations involving, e.g., not only Δj=-1 but also, in some cases, Δj=-2.[25] Furthermore, the vibro-rotational relaxation process also opens the way to new possible energy exchange routes, due to the coupling between the vibrational and rotational motions.

Finally, it is worth noting that the limited number of theoretical results available on the vibrational and rotational relaxation of molecules in HeNDs show a wide variety of values for the relaxation times.[16,24,25] Moreover, on the basis of the amount of excitation energy that has to be released from the molecule to the helium and the time required for this to occur, the theoretical results suggest that vibrational energy transfer is more efficient than rotational energy transfer.

4. Summary and conclusions

The vibrational energy relaxation of a homonuclear diatomic molecule (X_2) inside a superfluid helium nanodroplet (T=0.37 K; finite quantum solvent) has been investigated using a hybrid quantum approach recently proposed by us. The helium and the X_2 molecule have been described using TDDFT and standard quantum dynamics methods, respectively; and we have followed the same mathematical strategy for the time propagation as in a previous work of our group.[16]

This contribution complements and extends our recent work,[16] where the VER in HeNDs was studied for the first time, considering the I_2 molecule as initial example. Here, taking as a reference the I_2(X)@(^{4}He)$_{100}$ system, we have obtained a deeper insight into the vibrational relaxation dynamics through the analysis of the influence of the nanodroplet size (N=50, 100, 150 and 200), molecule-helium interaction potential energy ($V = xV_{I_2-He}$ with x=0.50, 0.75, 1.00, 1.25 and 1.50 and N=100) and v=1-v=0 vibrational energy gap ($v_e = xv_{e,I_2}$ with x=0.75, 1.00, 1.25 and 1.50 and N=100) on this relaxation process.

The present results show that the nanodroplet size has a little effect on the VER dynamics, as the interaction between the molecule and the liquid helium is mainly due

to the first solvation shell (due to the relatively large I_2-He interaction this solvation shell is fully formed for all the nanodroplet sizes studied). The interaction potential energy and the energy gap have an important and comparable influence on the VER time properties (global relaxation time, lifetime and transition time), which decrease in a significant way as the interaction potential energy is stronger and the vibrational energy gap decreases.

An interpretation based on the expected value, during the transition time, of the coupling term between the two vibrational levels involved, $\langle V_{01}^2 \rangle$, and on the oscillator velocity (that is proportional to $\nu_e^{1/2}$) has been attempted. As the interaction energy becomes stronger the relaxation times decrease in a significant way, according to a linear dependence of the inverse of the relaxation times with respect to the $\langle V_{01}^2 \rangle$ coupling term. The relaxation times also decrease in an important manner when the v=1-v=0 energy gap diminishes and they follow a linear dependence with respect to the v=1-v=0 energy difference.

Furthermore, the molecule-helium interaction energy is hardly modified during the relaxation process, but it shows oscillations during the transition, which means that the nanodroplet structure is essentially unchanged. More theoretical and experimental research on this interesting relaxation process in HeNDs, about which our knowledge is still very scarce, is desirable.

There are no conflicts of interest to declare.

Acknowledgements

This work has been supported by the Spanish Ministry of Science, Innovation and Universities (project ref. MDM-2017-0767) M. B.-J. acknowledges the University of Barcelona for a PhD research grant, and we also want to acknowledge some support from the Autonomous Government of Catalonia (project ref. 2017SGR 348). Thanks are also given to Dr. Arnau Vilà for useful discussions on vibrational relaxation in helium nanodroplets. We dedicate this work to the memory of our dear friend and colleague Prof. Fernando Castaño (University of the Basque Country), who made numerous

View Article Online
DOI: 10.1039/D1CP03629G

contributions in the field of molecular spectroscopy, including systems where van der Waals interactions play an important role.

References

[1] R. D. Levine, *Molecular reaction dynamics,* Cambridge University Press, Cambridge, 2005.

[2] D. W. Oxtoby, Vibrational population relaxation in liquids, *Adv. Chem. Phys.,* 1981, **47,** 487-519.

[3] D. W. Oxtoby, Vibrational relaxation in liquids: quantum states in a classical bath, *J. Phys. Chem.,* 1983, **87,** 3028-3033.

[4] Q. Shi and E. Geva, Semiclassical theory of vibrational energy relaxation in the condensed phase, *J. Phys. Chem. A,* 2003, **207,** 9059-9069.

[5] A. Nitzan, *Chemical dynamics in condensed phases,* Oxford University Press, Oxford, 2006.

[6] B. Bagchi, *Molecular relaxation in liquids,* Oxford University Press, Oxford, 2012.

[7] J. C. Owrutsky, D. Raftery and R. M. Hochtrasser, Vibrational relaxation dynamics in solutions, *Annu. Rev. Phys. Chem.,* 1994, **45,** 519-555.

[8] *Ultrashort laser pulses. Generation and applications,* ed. W. Kaiser, Springer, Berlin, 1993.

[9] S. Mukamel, *Principles of nonlinear optical spectroscopy,* Oxford University Press, New York, 1999.

[10] A. Tokmakoff, Time-dependent quantum mechanics and spectroscopy, https://tdqms.uchicago.edu/page/tdqms-notes accessed January 2019.

[11] J. S. Bader and B. J. Berne, Quantum and classical relaxation rates from classical simulations, *J. Chem. Phys.,* 1994, **100,** 8359-8366.

[12] J. P. Toennies and A. F. Vilesov, Superfluid helium droplets: a uniquely cold nanomatrix for molecules and molecular complexes, *Angew. Chem., Int. Ed.,* 2004, **43,** 2622-2648.

[13] M. Y. Choi, G. E. Douberly, T. M. Falconer, W. K. Lewis, C. M. Lindslay, J. M. Merritt, P. L. Stiles and R. E. Miller, Infrared spectroscopy of helium nanodroplets: novel methods for physics and chemistry, *Int. Rev. Phys. Chem.,* 2006, **25,** 15-75.

[14] A. Slenczka and J. P. Toennies, in *Low Temperature and Cold Molecules,* ed. I. W. M. Smith, Imperial College Press, London, 2008, pp. 345-392 and references therein.

[15] S. Yang and A. M. Ellis, Helium droplets: a chemistry perspective, *Chem. Soc. Rev.,* 2013, **42,** 472-484.

[16] A. Vilà, M. Paniagua and M. González, Vibrational energy relaxation dynamics of diatomic molecules inside superfluid helium nanodroplets. The case of the I_2 molecule, *Phys. Chem. Chem. Phys.,* 2018, **20,** 118-130.

View Article Online
DOI: 10.1039/D1CP03629G

[17] A. Vilà, M. González and R. Mayol, Photodissociation dynamics of homonuclear diatomic molecules in helium nanodroplets. The case of $Cl_2@(4He)_N$, *J. Chem. Theory Comput.,* 2015, **11,** 899-906.

[18] A. Vilà, M. González and R. Mayol, Quantum interferences in the photodissociation of $Cl_2(B)$ in superfluid helium nanodroplets $(^4He)_N$, *Phys. Chem. Chem. Phys.,* 2015, **17,** 32241-32250.

[19] A. Vilà and M. González, Mass effects in the photodissociation of homonuclear diatomic molecules in helium nanodroplets: inelastic collision and viscous flow energy exchange regimes, *Phys. Chem. Chem. Phys.,* 2016, **18,** 27630-27638.

[20] A.Vilà, M. González and R. Mayol, Quantum dynamics of the pick up process of atoms by superfluid helium nanodroplets: the $Ne+(^4He)_{1000}$ system, *Phys. Chem. Chem. Phys.,* 2016, **18,** 2006-2014.

[21] M. Blancafort-Jorquera, A. Vilà and M. González, Quantum-classical dynamics of the capture of neon atoms by superfluid helium nanodroplets, *Phys. Chem. Chem. Phys.,* 2018, **20,** 29737-29753.

[22] A. Vilà and M. González, Reaction dynamics inside superfluid helium nanodroplets: the formation of Ne_2 molecule from $Ne+Ne@(^4He)_N$, *Phys. Chem. Chem. Phys.,* 2016, **18,** 31869-31880.

[23] M. Blancafort-Jorquera, A. Vilà and M. González, Quantum-classical approach to the reaction dynamics in a superfluid helium nanodroplet. The Ne_2 dimer and Ne-Ne adduct formation reaction Ne + Ne-doped nanodroplet, *Phys. Chem. Chem. Phys.,* 2019, **21,** 24218-24231.

[24] M. Blancafort-Jorquera, A. Vilà and M. González, Rotational energy relaxation quantum dynamics of a diatomic molecule in a superfluid helium nanodroplet and study of the hydrogen isotopes case, *Phys. Chem. Chem. Phys.,* 2019, **21,** 21007-21021.

[25] E. Sanchez, Rotational energy relaxation in superfluid helium nanodroplets. The case of HCl and isotopic variants, Master thesis, University of Barcelona, 2021.

[26] A. Vilà and M. González and R. Mayol, Relaxation dynamics of helium nanodroplets after photodissociation of a dopant homonuclear diatomic molecule. The case of $Cl_2@(^4He)_N$, *Phys. Chem. Chem. Phys.,* 2016, **18,** 2409-2416.

[27] M. P. de Lara-Castells, A. W. Hauser and A. O. Mitrushchenkov, Ab initio confirmation of a harpoon-type electron transfer in a helium droplet, *J. Phys. Chem. Lett.*, 2017, **8**, 4284-4288.

View Article Online
DOI: 10.1039/D1CP03629G

[28] J. Tiggesbäumker and F. Stienkemeier, Formation and properties of metal clusters isolated in helium droplets, *Phys. Chem. Chem. Phys.,* 2007, **9,** 4748-4770.

[29] S. Yang, A. M. Ellis, D. Spence, C. Feng, A. Boatwright, E. Latimer and C. Binns, Growing metal nanoparticles in superfluid helium, *Nanoscale,* 2013, **5,** 11545-11553.

[30] M. Lasserus, M. Schnedlitz, D. Knez, R. Messner, A. Schiffmann, F. Lackner, A. W. Hauser, F. Hofer and W. E. Ernst, Thermally induced alloying processes in a bimetallic system at the nanoscale: AgAu sub-5 nm core–shell particles studied at atomic resolution, *Nanoscale*, 2018, **10**, 2017-2024.

[31] M. Schnedlitz, R. Fernandez-Perea, D. Knez, M. Lasserus, A. Schiffmann, F. Hofer, A. W. Hauser, M. P. de Lara-Castells and W. E. Ernst, Effects of the core location on the structural stability of Ni—Au core—shell nanoparticles, *J. Phys. Chem. C*, 2019, **123**, 20037-20043.

[32] M. Schnedlitz, D. Knez, M. Lasserus, F. Hofer, R. Fernández-Perea, A. W. Hauser, M. P. de Lara-Castells and W. E. Ernst, Thermally induced diffusion and restructuring of iron triade (Fe, Co, Ni) nanoparticles passivated by several layers of gold, *J. Phys. Chem. C*, 2020, **124**, 16680-16688.

[33] L. F. Gomez, E. Loginov and A. F. Vilesov, Traces of vortices in superfluid helium droplets, *Phys. Rev. Lett.,* 2012, **108,** 155302.

[34] E. Latimer, D. Spence, C. Feng, A. Boatwright, A. M. Ellis and S. Yang, Preparation of ultrathin nanowires using superfluid helium droplets, *Nano Lett.,* 2014, **14,** 2902-2906.

[35] R. Zadoyan, J. Almy and V. A. Apkarian, Lattice dynamics from the 'eyes' of the chromophore. Real-time studies of I_2 isolated in rare gas matrices, *Faraday Discuss.,* 1997, **108,** 255-269.

[36] J. Almy, K. Kizer, R. Zadoyan and V. A. Apkarian, Resonant Raman, hot, and cold luminiscence of iodine in rare gas matrices, *J. Phys. Chem. A,* 2000, **104,** 3508-3520.

[37] M. Karavitis, R. Zadoyan and V. A. Apkarian, Time resolved coherent anti-Stokes Raman scattering of I_2 isolated in matrix argon: vibrational dynamics on the electronic ground state, *J. Chem. Phys.,* 2001, **114,** 4131-4140.

[38] Z. Bihary, M. Karavitis and V. A. Apkarian, Onset of decoherence: six-wave mixing measurements of vibrational decoherence on the excited electronic state of I_2 in solid argon, *J. Chem. Phys.,* 2004, **120,** 8144-8156.

[39] M. Karavitis, T. Kumada, I. U. Goldschleger and V. A. Apkarian, Vibrational dissipation and dephasing of $I_2(v = 1\text{-}19)$ in solid Kr, *Phys. Chem. Chem. Phys.,* 2005, **7,** 791-796.

View Article Online
DOI: 10.1039/D1CP03629G

[40] T. Kiviniemi, J. Aumanen, P. Myllyperkiö, V. A. Apkarian and M. Petterson, Time-resolved coherent anti-Stokes Raman scattering measurements of I_2 in solid Kr: vibrational dephasing on the ground electronic state at 2.6-32 K, *J. Chem. Phys.,* 2005, **123,** 064509.

[41] M. Gruebele and A. H. Zewail, Femtosecond wave packet spectroscopy: coherences, the potential, and structural determination, *J. Chem. Phys.,* 1993, **98,** 883-902.

[42] Q. Liu, C. Wan and A. H. Zewail, Solvation ultrafast dynamics of reactions 13. Theoretical and experimental studies of wave packet reaction coherence and its density dependence, *J. Phys. Chem. A,* 1996, **100,** 18666-18682.

[43] J.-K. Wang, Q. Liu and A. H. Zewail, Solvation ultrafast dynamics of reactions 9. Femtosecond studies of dissociation and recombination of iodine in argon clusters, *J. Chem. Phys.,* 1995, **99,** 11309-11320.

[44] K. P. Huber and G. Herzberg, *Molecular spectra and molecular structure IV. Constants of diatomic molecules,* Van Nostrand Reinhold Co., New York, 1979.

[45] D. W. Schwenke and D. G. Truhlar, The effect of Wigner singularities on low-temperature vibrational relaxation rates, *J. Chem. Phys.,* 1985, **83,** 3454-3461.

[46] Z. Ma, S. D. Jons, C. F. Giese and W. R. Gentry, Crossed beam studies of state-to-state vibrational energy transfer from the $v = 5$ excited state of $I_2(X^1\Sigma_g^+)$ prepared by stimulated emission pumping, *J. Chem. Phys.,* 1991, **94,** 8608-8610.

[47] M. L. Nowlin and M. C. Heaven, Energy transfer rate constants for highly excited rovibrational levels of $I_2(X)$, *J. Chem. Phys.,* 1993, **99,** 5654-5660.

[48] H. J. Liu, S. H. Pullen, L. A. Walker II and R. J. Sension, The vibrational relaxation of $I_2(X^1\Sigma_g^+)$ in mesitylene, *J. Chem. Phys.,* 1998, **108,** 4992-5001.

[49] S. Li, and W. H. Thomson, Simulations of the vibrational relaxation of I_2 in Xe, *J. Phys. Chem. A,* 2003, **107,** 8696-8704.

[50] S. Li and W. H. Thomson, Molecular dynamics simulations of the vibrational relaxation of I_2 in Xe on an ab initio-based potential function, *Chem. Phys. Lett.,* 2004, **383,** 326-331.

[51] S. A. Egorov and J. L. Skinner, A theory of vibrational relaxation in liquids, *J. Chem. Phys.,* 1996, **105,** 7047-7058.

[52] D. W. Miller and S. A. Adelman, Time correlation function approach to liquid phase vibrational energy relaxation: dihalogen solutes in rare gas solvents, *J. Chem. Phys.,* 2002, **117,** 2672-2687.

View Article Online
DOI: 10.1039/D1CP03629G

[53] S. A. Adelman, R. Muralidhar and R. H. Stote, Time correlation function approach to vibrational energy relaxation in liquids: revised results for monoatomic solvents and a comparison with the isolated binary collision model, *J. Chem. Phys.,* 1991, **95,** 2783-2751.

[54] J. K. Brown, C. B. Harris and J. C. Tully, Studies of chemical reactivity in the condensed phase IV. Density dependent molecular dynamics simulations of vibrational relaxation in simple liquids, *J. Chem. Phys.,* 1988, **89,** 6687-6696.

[55] D. J. Nesbitt and J. T. Hynes, Vibrational energy transfer from highly excited anharmonic oscillators. Dependence on quantum state and interaction potential, *J. Chem. Phys.,* 1982, **76,** 6002-6014.

[56] R. H. Stote and S. A. Adelman, Theory of vibrational energy relaxation in liquids: diatomic solutes in monatomic solvents, *J. Chem. Phys.,* 1988, **88,** 4415-4420.

[57] R. E. Larsen and R. M. Stratt, Instantaneous pair theory for high-frequency vibrational energy relaxation in fluids, *J. Chem. Phys.,* 1999, **110,** 1036-1052.

[58] A. Bastida, C. Cruz, J. Zúniga, A. Requena and B. Miguel, Surface hopping simulation of the vibrational relaxation of I_2 in liquid xenon using the collective probabilities algorithm, *J. Chem. Phys.,* 2004, **121,** 10611-10622.

[59] M. E. Paige, D. J. Russell and C. B. Harris, Studies of chemical reactivity in the condensed phase II, Vibrational relaxation of iodine in liquid xenon following geminate recombination, *J. Chem. Phys.,* 1986, **85,** 3699-3700.

[60] M. E. Paige and C. B. Harris, Ultrafast studies of chemical reactions in liquids: validity of gas phase vibrational relaxation models and density dependence of bound electronic state lifetimes, *J. Chem. Phys.,* 1990, **149,** 37-62.

[61] K. Nauta and R. E. Miller, Solvent mediated vibrational relaxation: superfluid helium droplet spectroscopy of HCN dimer, *J. Chem. Phys.,* 1999, **111,** 3426-3433.

[62] S. Grebenev, M. Havenith, F. Madeja, J. P. Toennies and A. F. Vilesov, Microwave-infrared double resonance spectroscopy of an OCS molecule inside a ^{4}He droplet, *J. Chem. Phys.,* 2000, **113,** 9060-9066.

[63] K. Nauta and R. E. Miller, Metastable vibrationally excited HF ($v = 1$) in helium nanodroplets, *J. Chem. Phys.,* 2000, **113,** 9466-9469.

[64] K. Nauta and R. E. Miller, Vibrational relaxation of Ne, Ar, Kr-HF ($v = 1$) binary complexes in helium nanodroplets, *J. Chem. Phys.,* 2001, **115,** 4508-4514.

View Article Online
DOI: 10.1039/D1CP03629G

[65] B. Grüner, M. Schlesinger, P. Heister, W. T. Strunz, F. Stienkemeier and M. Mudrich, Vibrational relaxation and dephasing of Rb_2 attached to helium nanodroplets, *Phys. Chem. Chem. Phys.,* 2011, **13,** 6816-6826.

[66] P. Claas, G. Droppelmann, C. P. Schulz, M. Mudrich and F. Stienkemeier, Wave packet dynamics on triplet states of Na_2 attached to helium nanodroplets, *J. Phys. Chem. A,* 2007, **111,** 7537-7541.

[67] M. Schlesinger, M. Mudrich, F. Stienkemeier and W. T. Strunz, Dissipative vibrational wave packet dynamics of alkali dimers attached to helium nanodroplets, *Chem. Phys. Lett.,* 2010, **490,** 245-248.

[68] J. H. Reho, J. Higgins, M. Nooijen, K. K. Lehmann, G. Scoles and M. Gutowski, Photoinduced nonadiabatic dynamics in quartet Na_3 and K_3 formed using helium nanodroplet isolation. *J. Chem. Phys.,* 2001, **115,** 10265-10274.

[69] B. Shepperson, A. A. Søndergaard, L. Christiansen, J. Kaczmarczyk, R. E. Zillich, M. Lemeshko and H. Stapelfeldt, Laser-induced rotation of iodine molecules in helium nanodroplets: revivals and breaking free, *Phys. Rev. Lett.,* 2017, **118,** 203203.

[70] D. Mateo, A. Hernando, M. Barranco, E. Loginov, M. Drabbels and M. Pi, Translational dynamics of photoexcited atoms in ^{4}He nanodroplets: the case of silver, *Phys. Chem. Chem. Phys.,* 2013, **15,** 18388-18400.

[71] N. B. Brauer, S. Smolarek, E. Loginov, D. Mateo, A. Hernando, M. Pi, M. Barranco, W. J. Bruma and M. Drabbels, Critical Landau velocity in helium nanodroplets, *Phys. Rev. Lett.,* 2013, **111,** 153002.

[72] A. Leal, D. Mateo, A. Hernando, M. Pi and M. Barranco, Capture of heliophobic atoms by ^{4}He nanodroplets: the case of cesium, Phys. *Chem. Chem. Phys.,* 2014, **16,** 23206-23213.

[73] D. Mateo, F. Gonzalez and J. Eloranta, Rotational superfluidity in small helium nanodroplets, *J. Phys. Chem. A,* 2015, **119,** 2262-2270.

[74] F. Dalfovo, A. Lastri, L. Pricaupenko, S. Stringari and J. Treiner, Structural and dynamical properties of superfluid helium: a density-functional approach, *Phys. Rev. B: Condens. Matter Mater. Phys.,* 1995, **52,** 1193-1209.

[75] F. Ancilotto, M. Barranco, F. Caupin, R. Mayol and M. Pi, Freezing of ^{4}He and its liquid-solid interface from density functional theory, *Phys. Rev. B: Condens. Matter Mater. Phys.,* 2005, **72,** 214522.

[76] L. Delgado-Tellez, A. Valdés, R. Prosmiti, P. Villarreal and G. Delgado-Barrio, HeI_2 interaction potential based on an interpolation scheme, *Int. J. Quantum Chem.,* 2012, **112,** 2971-2975.

View Article Online
DOI: 10.1039/D1CP03629G

[77] M. Frigo and S. G. Johnson, The design and implementation of FFTW3, *IEE Proceedings,* 2005, **93,** 216-231.

[78] A. Ralston, in *Mathematical Methods for Digital Computers,* ed. A. Ralston and H.S. Wilf, John Wiley & Sons, New York, 1960, vol. 1, pp. 95-109.

[79] R. J. Thompson, Improving round-off in Runge-Kutta computations with Gill's method, *Commun. ACM,* 1970, *13,* 739-740.

[80] A. Vibók and G. G. Balint-Kurti, Parametrization of complex absorbing potentials for time-dependent quantum Dynamics, *J. Phys. Chem.,* 1992, **96,** 8712-8719.

[81] G. C. Schatz and M. A. Ratner, Quantum mechanics in chemistry, Dover, Mineola, 2002, pp. 70-74.

[82] M. P. de Lara-Castells, N. F. Aguirre, H. Stoll, A. O. Mitrushchenkov, D. Mateo and M. Pi, Communication: unraveling the ^{4}He droplet-mediated soft-landing from ab initio-assisted and time-resolved density functional simulations: Au@$^4He_{300}$/TiO_2(110), *J. Chem. Phys.*, 2015, **142**, 131101.

[83] F. Coppens, F. Ancilotto, M. Barranco, N. Halberstadt and M. Pi, Dynamics of impurity clustering in superfluid ^{4}He nanodroplets, *Phys. Chem. Chem. Phys.*, 2019, **21**, 17423-17432.